Wind and Structures, *Vol. 28, No. 6 (2019) 355-367*
DOI: https://doi.org/10.12989/was.2019.28.6.355

The effect of upstream low-drag vortex generators on juncture flows

Md.Y. Younis[*1], Hua Zhang[2], Bo Hu[3], Emad Uddin[4] and Jawad Aslam[4]

[1]*Department of Mechanical Engineering, Mirpur University of Science and Technology (MUST), Mirpur 10250 (AJK), Pakistan*
[2]*National Key Laboratory of Fluid Mechanics, Beihang University (BUAA), Beijing 100191, China*
[3]*Department of Engineering Mechanics, Shijiazhuang Tiedao University, Shijiazhuang 050043, HeBei, China*
[4]*Department of Mechanical Engineering, SMME, National University of Science and Technology (NUST), H-12, Islamabad, 46000, Pakistan*

(Received June 17, 2018, Revised February 6, 2019, Accepted February 10, 2019)

Abstract. Control of horseshoe vortex in the circular cylinder-plate juncture using vortex generator (VG) was studied at Re_D(where D is the diameter of the cylinder) = 2.05×10^5. Impact of a number of parameters e.g., the shape of the VG's, number of VG pairs (n), spacing between the VG and the cylinder leading edge (L), lateral gap between the trailing edges of a VG pair (g), streamwise gap between two VG pairs (S_{VG}) and the spacing between the two VG's in parallel arrangement (Z_{VG}) etc. were investigated on the horseshoe vortex control. The study is conducted using surface oil flow visualization and surface pressure measurements in low speed wind tunnel. It is observed that all the parameters studied have significant control effect, either by reduction in separation region or by lowering the adverse pressure along the symmetric axis upstream of the juncture.

Keywords: horseshoe vortex; low drag vortex generators; streamwise vortex; series arrangement of vortex generators; parallel arrangement of vortex generators

1. Introduction

When hindrances and obstacles come across the flowing fluid, some very complex flow structures form all around the obstacles (upstream, downstream and sidewise). The complex flow structures exert a number of adverse effects on the obstacle around which they are formed. The results of such flow structures on the obstacle appear in the form of vibration, noise, erosion etc. Some of the common flow structures around an obstacle when it is placed in a fluid stream are the wake flow (Karman Vortex), tip flow/vortex and the Horseshoe Vortex (Munson *et al.* 2009). All of the above flow structures are caused due to the separation of the boundary layer from some parts of the obstacle which results in such vortical flow structures. Horseshoe vortices are spawned due to the adverse pressure gradient offered by obstacles and encountered by the incoming boundary layer on its way. This vortical flow is then, convected downstream along the two sides of obstacles. (Younis *et al.* 2014)

Controlling the separated flows in various fluid mechanics applications have always remained a great challenge. The horseshoe vortex in junction is also an undesirable flow phenomenon in many situations which needs to be controlled in order to avoid the structural damage. This may be achieved by either using passive or active methods of flow control (Mohamed 2006).

A number of passive control methods have been developed. Some for specific applications concerning Juncture flows like fillets (Kubendran and Harvey 1985, Devenport *et al.* 1990, Zess and Thole 2002) (for aircrafts wings or for turbine blades junctures) or general purpose e.g. collars (Bijan 1990) etc. are studied. Fillets use the principle of reducing the adverse pressure gradients by making the juncture region more streamline according to the local flow conditions at that region. Studies suggest that the leading edge fillets (Kubendran and Harvey 1985, Devenport *et al.* 1990, Zess and Thole 2002) are more suitable for leading edge separation control than the fillet along the whole of the juncture (Devenport *et al.* 1990). The leading edge fillet greatly improves the stability of the flow close to juncture and uniformity of the wake. Leading edge fairing (Oudheusden *et al.* 2004) has also been successfully utilized to eliminate the horseshoe vortex with similar flow control mechanism to that of the fillets. Gupta (1987) used a delta wing like device in the base of the juncture region, and illustrated that the device acts as a barrier to vortex buildup and generates counter rotating pair of vortices with opposite sense of rotation to that of horseshoe vortex. Except Gupta, who used qualitative flow visualization technique for his analysis, no further detailed studies with this method are observed in available literature.

Variation in the shape of leading edge (Wei et al. 2008, Olcmen and Simpson 1994) of the obstacle plays an important role in horseshoe vortex modifications. Varying the airfoils (Olcmen and Simpson 1994) and the shapes of the cylinders (Wei *et al.* 2008) revealed that the sharp leading edge produces a weaker horseshoe vortex than a blunt one. This is due to the fact that sharp leading edges produce less adverse pressure gradients compared to the blunt counterparts.

Ribbed surfaces (Kairouz and Rahai 2005) upstream of the juncture also significantly reduce the horseshoe vortex strength and displace the separation point more close to the

∗Corresponding author, Dr.
E-mail: myyounis.me@must.edu.pk

http://www.techno-press.com/journals/was&subpage=7 ISSN: 1226-6116 (Print), 1598-6225 (Online)

juncture. Ribbed surfaces adds momentum to the near wall region with the introduction of force mixing of the free stream fluid into the boundary layer region which results in delayed separation compared to the baseline case.

Fencing is another important passive control method which is used to reduce the horseshoe vortex structure in the juncture region. Various ways of fencing (Liu *et al.* 2010, Kumar and Govardhan 2011) are used to reduce the strength of the horseshoe vortex system. Fences change the mechanism of flow near the juncture region thus the strength of the near wall vortical flow is reduced. Liu *et al.* (2014) also used vortex baffle to control the horseshoe vortex. Theberge and Ekmecki (2017) used triangular plate to control the horseshoe vortex.

An inclined thin rod (Wang *et al.* 2009) attached with the horseshoe vortex system also mitigates the vortex structure. Inclined rod separates the incoming boundary layer before it reaches the juncture, so as due to smaller adverse pressure gradient than that of the main juncture, the horseshoe vortex system in this case mitigates greatly. Two dimensional cavity (Kang *et al*. 2009) and a small cylinder placed in front of juncture (Younis *et al*. 2010) are some other passive control methods which are effective in horseshoe vortex control. An innovative idea of horseshoe vortex control is being carried out by Wang *et al*. (2011) who used Venturi tube for the passive suction of the incoming boundary layer removal. The method gives promising results on horseshoe vortex control and utilizes no energy for suction thus called “passive suction”.

In the active flow control methods, boundary layer flow suction (Philips *et al.* 1992, Jhonson *et al*. 1994, Seal and Smith 1999, Bloxham *et al.* 2008 and Liu and Song 2017) to control the horseshoe vortex has been employed. The purpose of all these studies is to remove the near wall boundary layer fluid along the surface of the plate in order to remove the span wise vorticity. This way the formation of horseshoe vortex has been suppressed, but the design of suction hole needs careful work such that the corners of the suction hole shouldn’t disturb the downstream flow. Blowing (Jhonson *et al*. 1994 and Bons *et al.* 2018) the high momentum fluid into the low momentum near wall flow has also been done to control the boundary layer separation in case of juncture flows. The control mechanism is based on the idea of energizing the near wall flow with the injection of high momentum fluid which effectively delays the separation.

Horseshoe vortex control by introducing stream wise vorticity (opposite to vorticity that of horseshoe vortex legs) in the downstream moving fluid before its interaction with the obstacle can be considered as an important control technique. Though a few studies (Doerffer *et al.* 2003, Andoh *et al.* 2009, 2010, Honami *et al*. 2011) are carried out where stream wise vortices are used to alter the horseshoe vortex, yet no focused and detailed work to author’s knowledge is found in the available literature. The above mentioned studies also provide very few information regarding the horseshoe vortex control using stream wise vortices, no parametric studies are available as well. The control method is passive and can be used in a number of applications such as flow separation on the airplane wings, vehicles, turbine blades, and bridge piers etc.

A detailed experimental study is presented, where a number of parameters of the passive vortex generators are be evaluated for the reduction in separation region of the juncture flows (using surface oil flow visualization) as well as in adverse pressure and its gradient (using surface pressure measurement) for a turbulent juncture flow.

2. Experimental setup

The experiments are conducted in the open test section, low speed wind tunnel facility of Institute of Fluid Mechanics in Beihang University (BUAA). The maximum attainable speed in the wind tunnel is 50ms^{-1}. Experiments are conducted at a fixed free stream velocity (U_∞) of 30 ms^{-1} at which the turbulence intensity was less than 0.3%. The test section of the tunnel is elliptic in shape with inlet section size of 1.02 m × 0.75 m and outlet size of 1.07 m × 0.81 m with length of the test section is 1.45 m.

A circular cylinder made of Plexi glass with diameter (D = 100 mm) and height (H = 250 mm) is mounted over a wooden flat plate of maximum width 1m and length of 1.3 m, to create a turbulent juncture flow. The cylinder is placed on the plate symmetric line with its center at 0.95 m from the plate leading edge so that the plate length based Reynolds number (at the position where later the leading edge of the cylinder is placed) is $Re = 1.85 \times 10^6$.

The calculated boundary layer thickness (δ) at the position where cylinder leading edge is placed is approximately 18.5 mm (when cylinder was not positioned). The schematic diagram of the setup is shown in Fig. 1. The Reynolds number based on cylinder diameter (D) in this study was $Re_D = 2.05 \times 10^5$. The wooden plate is made stepped in order to insert it inside the inlet of the test section and clamped with a fixture at 0° incidence angle. The plate has an elliptic (5:1) leading edge to avoid flow separation and a triangular trailing edge to avoid trailing edge effects. The plate was painted black to give a clear surface oil flow pattern when oil with bright tracer particles were applied on the plate surface for surface oil flow visualization. Tracer particles (Titanium-di-oxide) mixed with Silicon oil with Kerosene oil added for fluidity is brushed on the plate surface to get the surface flow pattern of the skin friction lines. A high resolution digital camera is used to capture the surface pattern. The average non-dimensional distance of the upstream separation line on the symmetric axis from the cylinder leading edge X_s (= x_s / D, where x_s is the distance between the upstream separation point on the symmetric axis to the leading edge of the cylinder) and average non-dimensional lateral distance of the upstream separation line from the cylinder side, Z_s (= z_s / D, where z_s is the distance between the separation line and the cylinder at 90° from the symmetric axis) as shown in Fig. 2, are obtained after repeating the experiments thrice for each case. The average non-dimensional distance of the upstream separation line on the symmetric axis from the cylinder leading edge X_s (= x_s / D, where x_s is the distance between the upstream separation point on the symmetric axis to the leading edge of the cylinder) and average non-dimensional lateral distance of

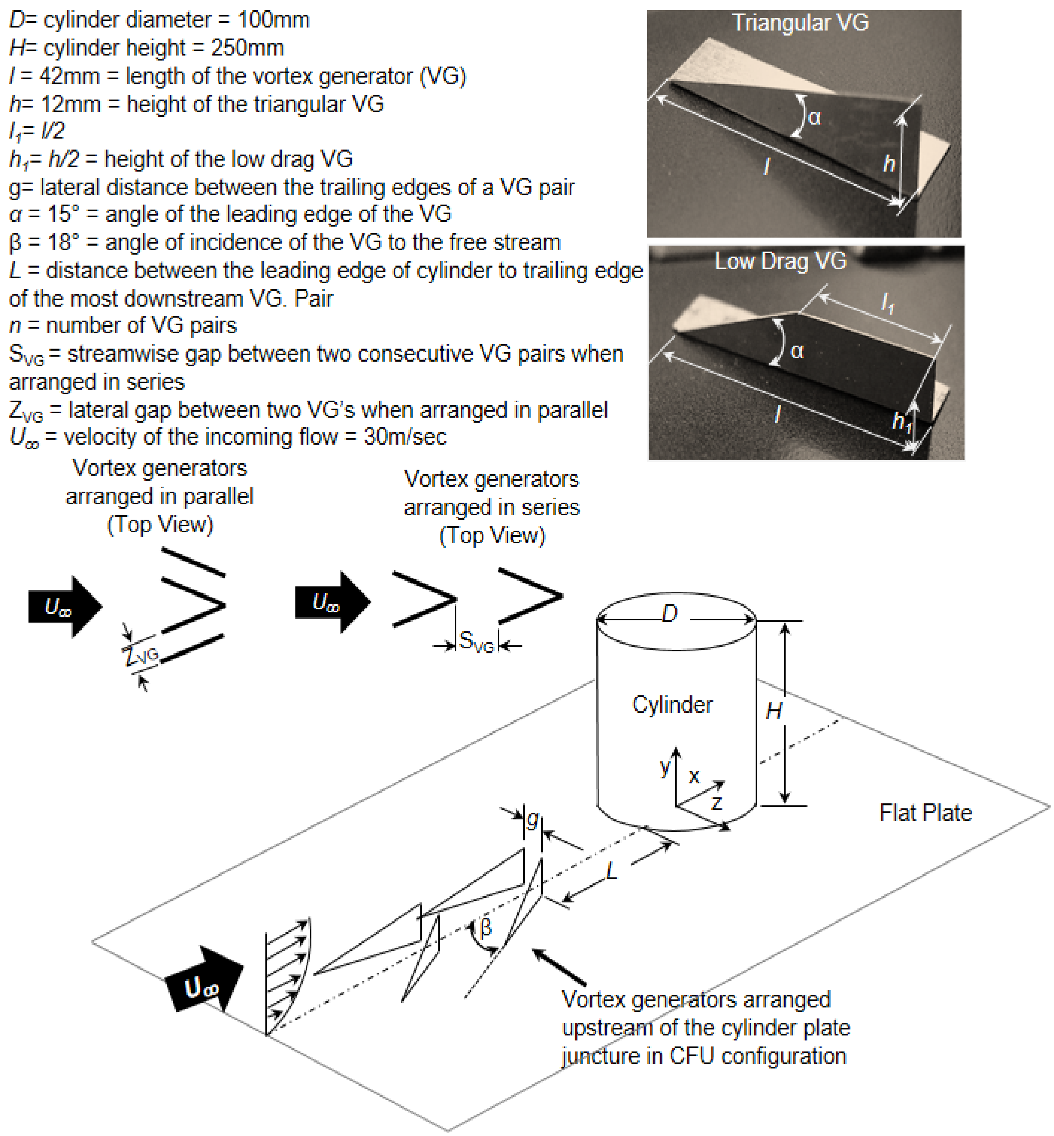

Fig. 1 Experimental setup and details of arrangement

the upstream separation line from the cylinder side, Z_s (= z_s / D, where z_s is the distance between the separation line and the cylinder at 90° from the symmetric axis) as shown in Fig. 2, are obtained after repeating the experiments thrice for each case. For the surface pressure measurements a total of 20 holes, each with diameter 1mm, are drilled in the plate along the upstream symmetric axis to cover a distance of 1.2D starting from the cylinder. The center to center gap between two consecutive holes was 6 mm and the first hole was drilled 3 mm upstream of the cylinder. Steel tubes of 1mm external and 0.7 mm internal diameter are inserted in the holes to measure the surface pressure, one end of steel tubes is connected to the pressure measuring system, NetScnner System 9816/98RK-1, using plastic tubes of maximum length of 1.5 m. The system has an accuracy of the ± 0.05% with maximum data sampling frequency of 100Hz. The time averaged surface pressure was measured for each pressure scanner for 600, 1000, 2000 and 5000 samples and found results didn't alter much in each case. Coefficient of pressure (C_p) was obtained for all the pressure ports for the flat plate without the cylinder fixed on it. The C_p for all the ports was found within the range ±0.01, as it should be for a flat plate boundary layer with no adverse pressure gradient. For the control of turbulent juncture flows, passive vortex generators (VG) of two shapes, a triangular and a low drag are used, as shown in Fig. 1. Both vortex generators used in the study are made of 0.5 mm thick metal sheet. Low profile vortex generator is made by cutting the upper half of the triangular vortex generator so the height for low profile VG is half that of the triangular VG. The length of each VG is 44 mm with height h = 12 mm and h = 6 mm for triangular and low profile VG, respectively. The swept angle for both VG's is fixed (α = 15°). The vortex generators are sticked to the flat plate upstream of the juncture on the symmetric axis with the help of thin double tape of thickness less than 0.5 mm.

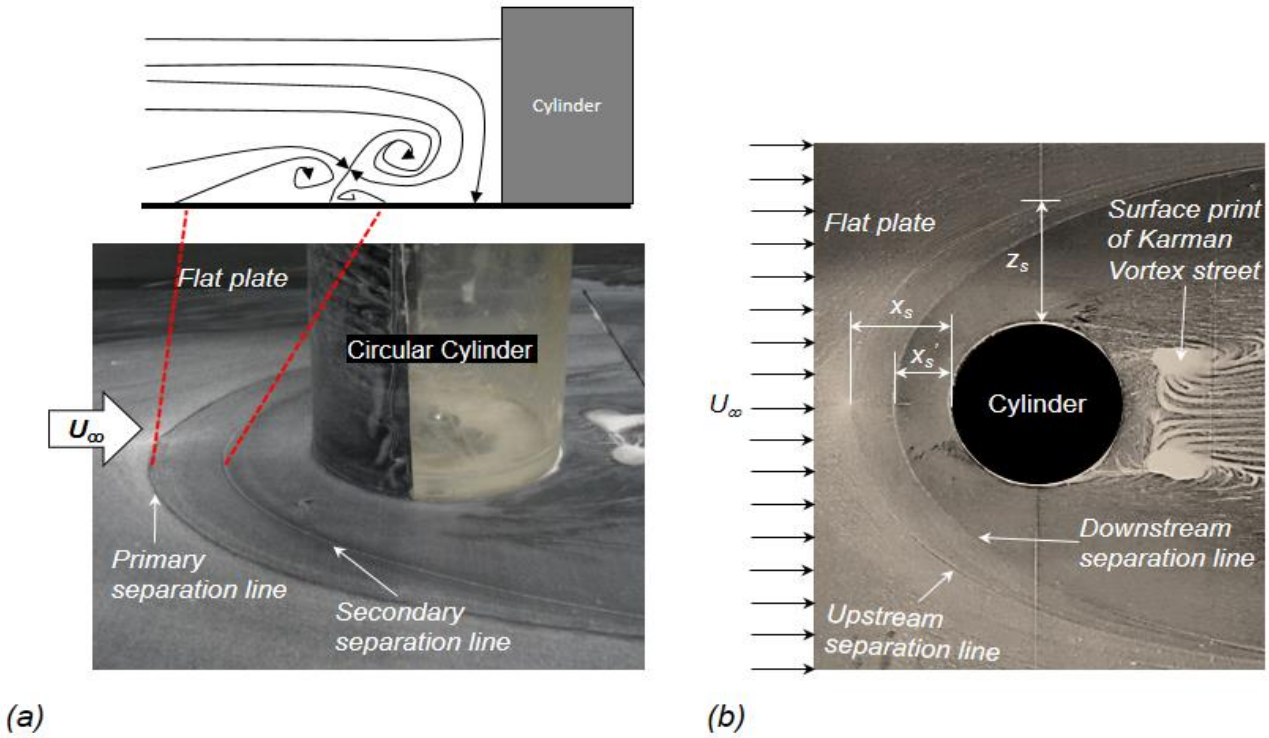

Fig. 2 (a) Flat plate and cylinder junction with surface print of the three dimensional flow separation and (b) Surface print of different flow structures on the plate around the juncture nomenclature used to measure the separation region in the streamwise and lateral directions

The vortex generators are placed upstream of the juncture symmetrically in common flow up (CFU) configuration (shown in Fig. 1) with incidence angles of $\beta = \pm 18^{\circ}$. The vortex generators, apart from the shape, will be analyzed for a number of parameters depending upon their arrangement in which they are fixed upstream on the juncture. These include; (1) the distance between the leading edge of the cylinder and the trailing edge of the near most vortex generators (L), (2) the lateral gap between the trailing edges of the VG when arranged in pair (g), (3) number of VG pairs (n), (4) streamwise gap between two consecutive VG pairs when arranged in series (S_{VG}) and (5) lateral gap between two VGs when arranged in parallel (Z_{VG}) as labeled in Fig. 1.

3. Results and discussion

The results of the experimentation conducted in this study is divided into two parts, the first is the flow visualization conducted using surface oil flow and the second is surface pressure measurement. Both will be explained separately in two sections.

3.1 Surface oil flow visualization

The incoming boundary layer flow when experiences the adverse pressure of the cylinder will separate from the surface of the plate and rollup to form the horseshoe vortex structure. The spatial horseshoe vortex structure incurred from the surface print of the oil flow pattern is sketched in Fig. 2(a). The result is found comparable to that of Baker (1980) and Zhang (2012) for turbulent flow conditions. The separation length (distance between the primary separation point to the leading edge of the cylinder along the upstream symmetric axis) is represented with X_S while the separation length between the primary separation line and side of the cylinder with Z_S, as shown in Fig. 2(b). In order to analyse the effect of the control technique on the separation region, surface oil flow visualization is conducted for juncture with and without the vortex generators. The results for three representative cases (Fig. 3), baseline (without control) Fig. 3(a), control using two Low drag VG pairs (n=2, L=2D, g=0, S_{VG}=0) arranged in series (Fig. 3(b)) and control using two Low drag VG pairs (n=2, L=2D, g=0, Z_{VG}=4h) arranged in parallel (Fig. 3(c)) are presented for reference. In order to facilitate the direct comparison, same scale is used for the three cases.

For the baseline case (Fig. 3(a)), there are two clear separation lines around the cylinder on the plate surface. The primary separation line, starts from the most upstream singular point on the symmetric axis at a distance X_S = 0.6 and convects downstream along the two sides of the juncture with a distance Z_S = 0.76 (shown in Fig. 3(a)). The separation region thus expands on its way downstream and the two separation lines gets closer. A clear symmetric surface print of the Karman vortex structure encompassing two large recirculating zones is observed in the downstream base region of the juncture.

The effect of control (reduction in separation region) has clearly been observed in Figs. 3(b) and 3(c). The separation region has shrunk both in the streamwise and lateral directions. The distance X_S has reduced from 0.6 for the baseline case (Fig. 3(a)) to 0.32 for the case when vortex generators are applied in series (Fig. 3(b). Z_S on the other hand has lessened to 0.42 from the baseline case value of 0.76. The two separation lines surface pattern has also reduced to a single separation line. The separation lines are also not as vivid as were in baseline case, which possibly is due to weak separation in the case under discussion compare to the reference baseline case. The Karman vortex pattern in the base region of plate cylinder juncture is also found narrowed to a very small area close to the symmetric line. This shows that the vortex generator not only reduce the separation region of HSV but also has promising control effect on the wake region close to the wall as well.

The separation region upstream of the juncture has a complex surface pattern when vortex generators are applied in parallel. Interaction of the two streamwise vortices, originating from two VGs from the same side of the symmetric axis, has led to a symmetric twin peak surface structure as observed in Fig. 3(c). A primary separation line has been extended towards the symmetric axis to draw the approximate separation length, and drawn using a white dashed line. Both, primary and secondary separation lines were observed thick and clear, this indicates a strong separation for both lines. The approximate separation distance along the symmetric axis (X_S) is measured to be 0.52, contrariwise Z_S = 0.27 is measured for this case. The surface print of the Von Karman vortex in the rear of the cylinder is also observed very small. No large rotating structures are observed as were found in baseline case (Fig. 3(a)).

Comparing the surface oil flow results for two different arrangements, the series and parallel, it is observed that the former is effective in reducing the upstream separation region (X_S) while later exhibits strong reduction in lateral direction (Z_S). Effect of different parameters e.g. shape of VG pairs, *n*, *L*, *g*, and S_{VG} for series arrangement and *n* and Z_{VG} for parallel arrangement, on the reduction in size of the separation zone is discussed below in detail based on surface oil flow visualization.

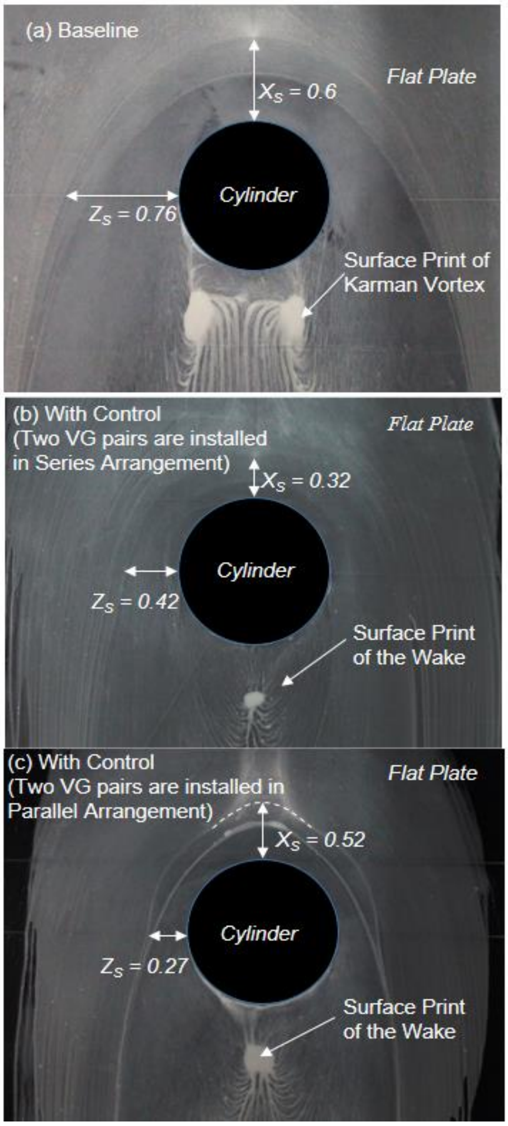

Fig. 3 Surface oil flow print of the flow structure around the juncture region (top view) (a) baseline case (b) with control when two pairs (n = 2) of low drag vortex generators are arranged in series and (c) with control when two pairs (n = 2) of low drag vortex generators are arranged in parallel upstream of the juncture, for (b) and (c) L=2D and flow is from top to bottom in the figures

3.1.1 Effect of the shape of the vortex generators in series arrangement

In order to evaluate the effect of the shape of the vortex generator, two profiles of VG are used as mentioned before, the triangular and the low drag. The low drag VG is half in maximum height (h_1) compare to that of triangular VG (*h*). X_S and Z_S for triangular and low drag VG pairs when arranged in series are presented in Fig. 4. The results revel that both X_S and Z_S are observed slightly larger for triangular VG compare to the low drag when single VG pair (*n=1*) is used (see Figs. 4(a1) and (a2)). As "*n*" is increased, not only the size of separation region (X_S and Z_S) reduces but the difference in results for triangular and low drag VG pairs also constricts.

3.1.2 Effect of the distance between the leading edge of cylinder to trailing edge of most downstream VG Pair (L) in series arrangement

Fig. 4 also shows the effect of *L* (Please see Fig. 1) on the reduction in separation region. Three values of *L* are used in this study that is *L*= D, 2D and 3D as shown in Fig. 4(a-c). It is found that at *L*= D (Fig. 4(a)), the separation region for both shapes (X_S = 0.77 and 0.85 for low drag and triangular VG pairs respectively) for *n*= 1, is larger than the baselines (*X*s = 0.6) case.

Z_S on the other hand has reduced slightly (Z_S = 0.67) for low drag VG but no reduction is observed for triangular VG pair (Z_S = 0.76) compare to the baseline case (Z_S = 0.76). Increasing the number of VG pairs to *n*=2, the X_S is found

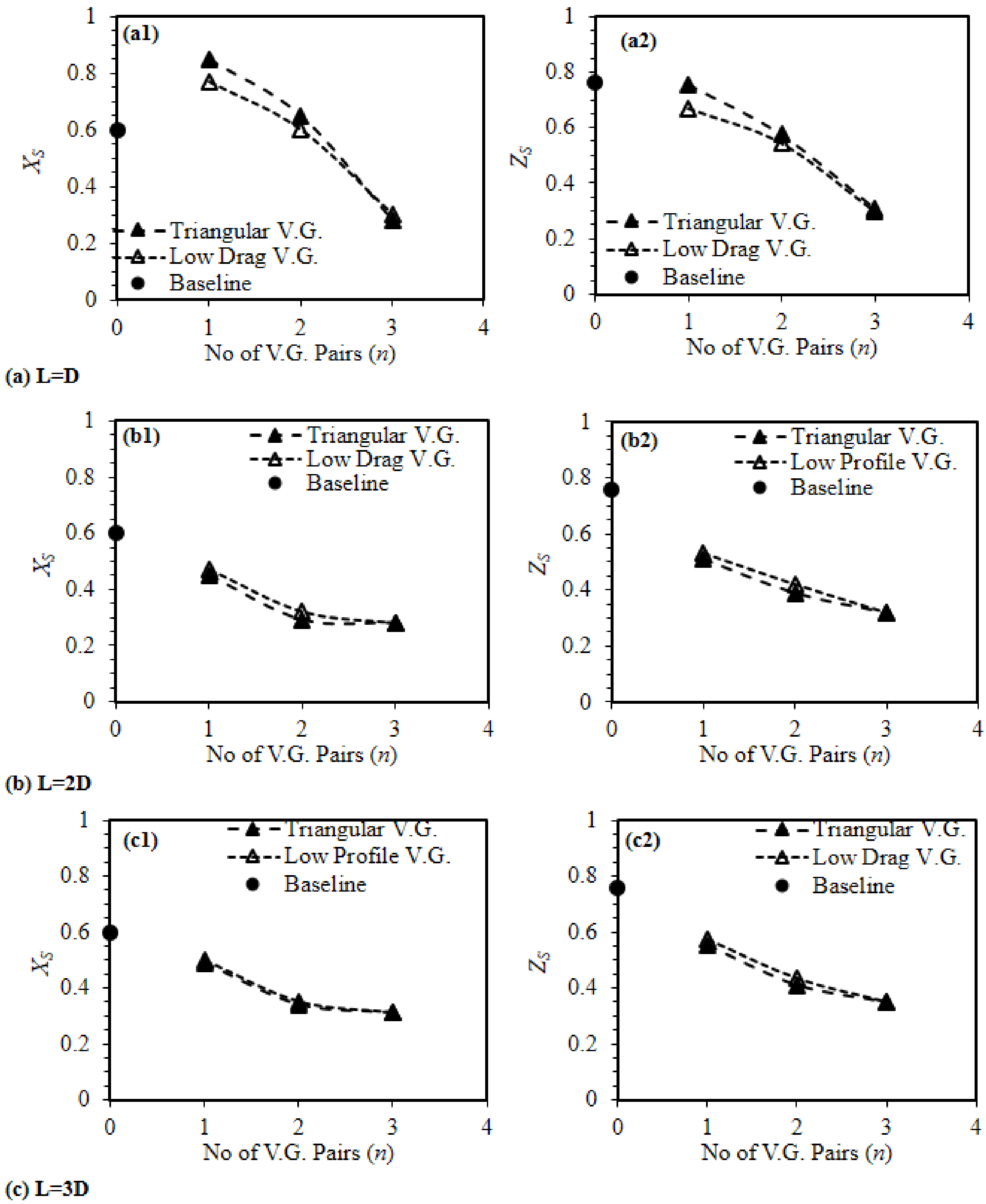

Fig. 4 Effect of gap between the trailing edge of the most downstream VGs and the leading edge of the cylinder (L) on upstream separation length (X_S) (left column) and on sidewise separation length (Z_S) (right column) (a) $L = D$, (b) $L = 2D$ *and* (c) $L = 3D$

0.65 and 0.6 respectively for triangular and low drag VG, while Z_S is found 0.57 and 0.54 respectively. Rising the number of VG pairs to n = 3, a sharp drop in both X_S and Z_S is observed. X_S drops to as low as 0.28 and 0.3 while Z_S drops to 0.31 and 0.3 respectively for triangular and low drag VG pairs. For n=3, the X_S for both VG pairs is observed half of that of the baseline case, on the other hand Z_S has dropped by 60% that of the baseline case.

At L= 2D (Fig. 4(b)), the separation region, X_S = 0.47 and 0.45 are observed for low drag and triangular VG pairs respectively, when n= 1. Z_S = 0.53 and 0.51 are observed respectively for low drag and triangular VG pairs. Both (X_S and Z_S) are observed smaller than the baseline case with a relatively large reduction in Z_S (reduction of ~32%) compare to the X_S (reduction of ~24%). Using n = 2 and L= 2D, the X_S drops to 0.32 and 0.29 respectively for low drag

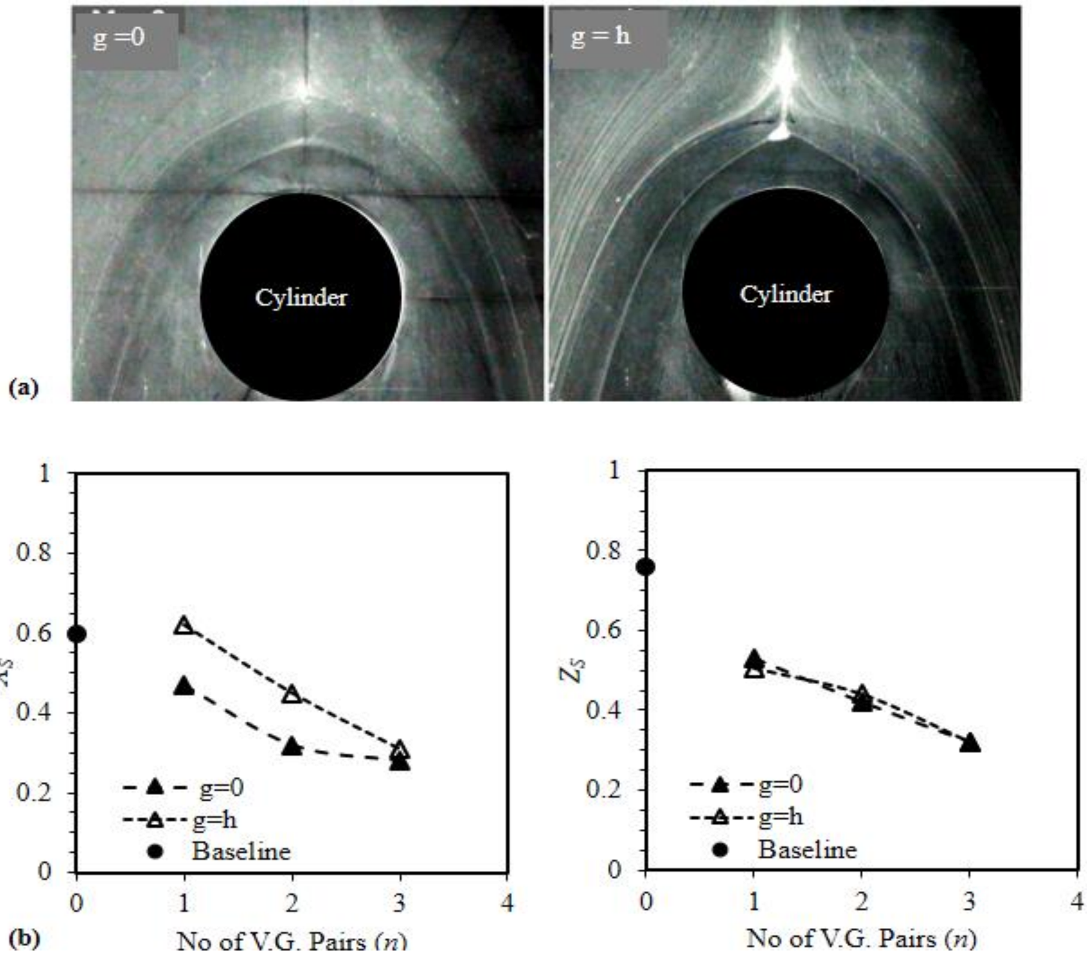

Fig. 5 Effect of distance between the trailing edges of the two vortex generators in a VG pair "*g*" on the flow separation region (a) surface oil flow visualization n =1, and (b) the variation in X_S and Z_S with varing n, the low drag vortex generator is placed at L=2D

and triangular VG, while Z_S = 0.42 and 0.39 are observed bringing the overall reduction to nearly 50% for both X_S and Z_S compare to the baseline case. Increasing the VG pairs to n =3 no further reduction is observed for X_S for triangular VG pairs while only a slight reduction (X_S = 0.28) for low drag VG pairs is observed compare to those at n =2 (X_S = 0.32). Z_S for both VG shapes drops to Z_S = 0.32. For n=3 the overall reduction in X_S is approximately 55% and for Z_S it is 58%. No significant enhancement in reduction in separation region is observed for n = 3 compare to n = 2 for both X_S and Z_S.

At L= 3D (Fig. 4(c)), the separation regions X_S and Z_S has increased slightly for both triangular and low drag VGs compare to the corresponding values at L= 2D for all "n". The X_S = 0.5, 0.35 and 0.31 is observed for n = 1, 2 and 3 respectively for low drag VG. For triangular VG on the other hand it is, X_S = 0.49, 0.34 and 0.31 respectively for n = 1, 2 and 3. In case of Z_S, for triangular VG, Z_S = 0.57, 0.43 and 0.35 and for low drag VG, Z_S = 0.55, 0.41 and 0.35 respectively for n =1, 2 and 3, in either case. The results shows that when VGs are placed at L= 3D, the control effect has lessened slightly compared to when placed at L= 2D. It is also observed that the control effect at L= D, *2D and* 3D with three VG pairs (n = *3*) for both triangular and low drag VG pairs were approximately same (X_S ~0.3 ± 0.03, and Z_S ~0.32 ± 0.03).

From this analysis it is concluded that two pairs of low profile VG (n =2) arranged in series at L = *2D* can provide a good combination of flow control (reduction in separation lengths) in the current situation

3.1.3 Effect of the spacing between the two Vortex generators in a pair (g) (series arrangement)

To evaluate the effect of the gap between the vortex generators arranged in pairs (g, shown in Fig. 1), g =0 and h are evaluated for n = 1, 2 and 3 at L= 2D.

Flow visualization results for the two cases (g = 0 and h) when n = 1 and L=2D are shown in Fig. 5(a). It is observed from the surface oil flow visualization (Fig. 5(a)), that the surface oil flow structure upstream of the juncture varies significantly by g. A beak like structure (bright pointed white region) is observed when g = h, while for g = 0 the surface structure was qualitatively alike that of the baseline. Despite the obvious difference in flow structure upstream of the juncture (intern the X_S), the impact is minimal on the separation length in the lateral direction (Z_S) Comparing the

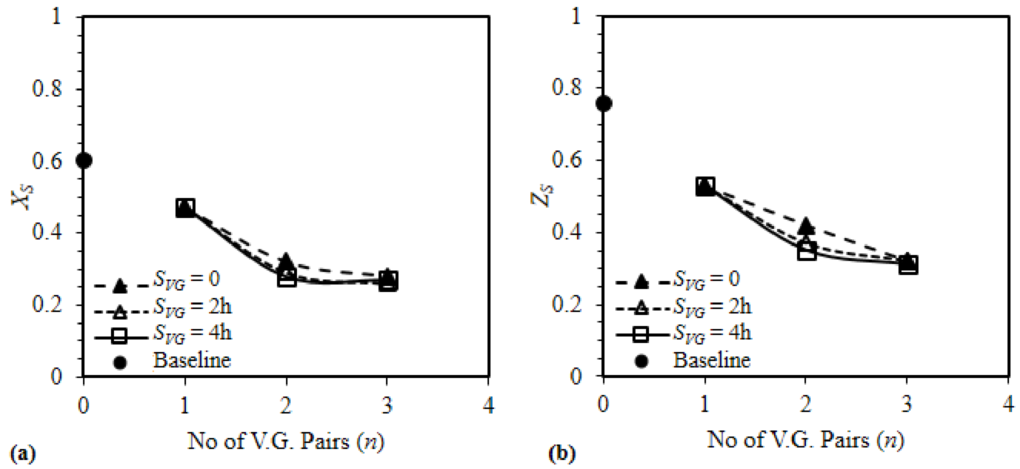

Fig. 6 Effect of distance between the two consecutive VG pairs in series arrangement (S_{VG}) on (a) the upstream separation length (X_S) and (b) the sidewise separation length (Z_S) of the juncture. Low drag vortex generator is placed at L=2D

separation length, X_S (Fig. 5(b)), it is observed that it extends to a large value (due to beak like structure) when g = h, compare to when g = 0. The beak gets weak gradually as the number of VG pairs are increased from n = 1 to 2, and then to 3 where X_S for both g = 0 and h is same (please see Fig. 5(b)). As already mentioned that separation length Z_S for n = 1 exhibits alike for both g = 0 and h, the same is observed for n = 2 and 3 as well. Due to the fact that the separation region upstream of the juncture becomes gratuitously complex with unequivocally no positive effect when gap (g) is present between the two VGs used in a pair, it should be avoided.

3.1.4 Effect of the streamwise gap between two VG pairs (S_{VG}) when arranged in series

Streamwise gap between two VG pairs ($S_{VG,}$ Please see Fig. 1) is also evaluated for possible impact on the reduction in separation region around the juncture. Three different gaps, S_{VG} = 0, 2h and 4h were tested with n = 1, 2 and 3 at L = 2D, and the results are shown in Fig. 6. Clearly both X_S and Z_S for n = 1 should be the same, as the minimum number of VG pairs needed to evaluate the effect must be n = 2. When n is increased to 2, both X_S and Z_S are altered slightly for varying $S_{VG.}$ X_S has lowered from 0.32 to 0.28 when S_{VG} is increased from 0 to 4h, when n = 2. A further increase in n = 3, shown that the gap S_{VG} makes no difference in separation length (X_S), and all the cases (S_{VG} = 0, 2h and 4h) have identical results. Z_S also shows a similar trend under the impact of increasing n and S_{VG} as is observed for X_S. For n = 2, the Z_S drops from 0.42 to 0.35 with increasing S_{VG} from 0 to 4h. Later, for n = 3, Z_S collapse again to same value (as shown in Fig. 6). It is concluded from the results that a streamwise gap S_{VG} = 4h gives the best results in the current scenario.

3.1.5 Effect of the lateral gap (Z_{VG}) between two co-rotating VGs on either side of symmetric axis when arranged in parallel

After the evaluation of various parameters for series arrangement of VG pairs for low drag VGs, they are also arranged in parallel and evaluated for possible control/reduction of juncture flow. Parallel arrangement of low drag VG pairs where n = 2 and L = 2D was already discussed in detail earlier in this section (see explanation for Fig. 3(c)). In the current section the variation in number of VG pairs (n =1, 2 and 3) with fixed Z_{VG} (= 4h) and L = 2D were investigated and the results are shown in Fig. 7. The surface oil flow visualization for the case when n = 2 and 3 are used, is shown in Fig. 7(a). Separation length Xs is observed increasing slightly from X_S = 0.49 when n = 1 to X_S = 0.52 when n = 2 with lateral spacing Z_{VG} = 4h. Increasing the number of VGs to n = 3, the separation length has further increase slightly to X_S = 0.56. Z_S on the other hand has shown significant reduction in when two (n = 2) VGs (Z_S = 0.27) on either side are used compare to the single (n = 1) VG (Z_S = 0.53). Increasing the number of VGs to n = 3, contributes nothing towards the reduction in separation region. This is due to the fact that the streamwise vortex generated by the outer most VG in case of n = 3, bypasses the juncture region without interacting the juncture flow (see Fig. 7(a)). It only interacts with the juncture flow as it moves towards the wake region, thus no further reduction in separation length Z_S compare to n = 2.

The effect of gap between the VGs (Z_{VG}) is also evaluated by changing the Z_{VG} from 4h to 2h (not shown here). Xs = 0.45 is observed for Z_{VG} = 2h compare to the X_S = 0.52 at Z_{VG} = 4h for n = 2. Conversely a large Z_S (= 0.355) is observed when Z_{VG} = 2h compare to Z_S (= 0.27) for Z_{VG} = 4h.

It is thus recommended that when the vortex generators were arranged in parallel, two VG (n = 2) with spacing Z_{VG} = 4h should be used.

3.2 Surface pressure measurements

The results obtained from surface oil flow visualization provide us with important basic idea about the reduction in separation region for horseshoe vortex. On the basis of these results, the surface pressure (C_P) measurements were planned and conducted to obtain a measure of the strength

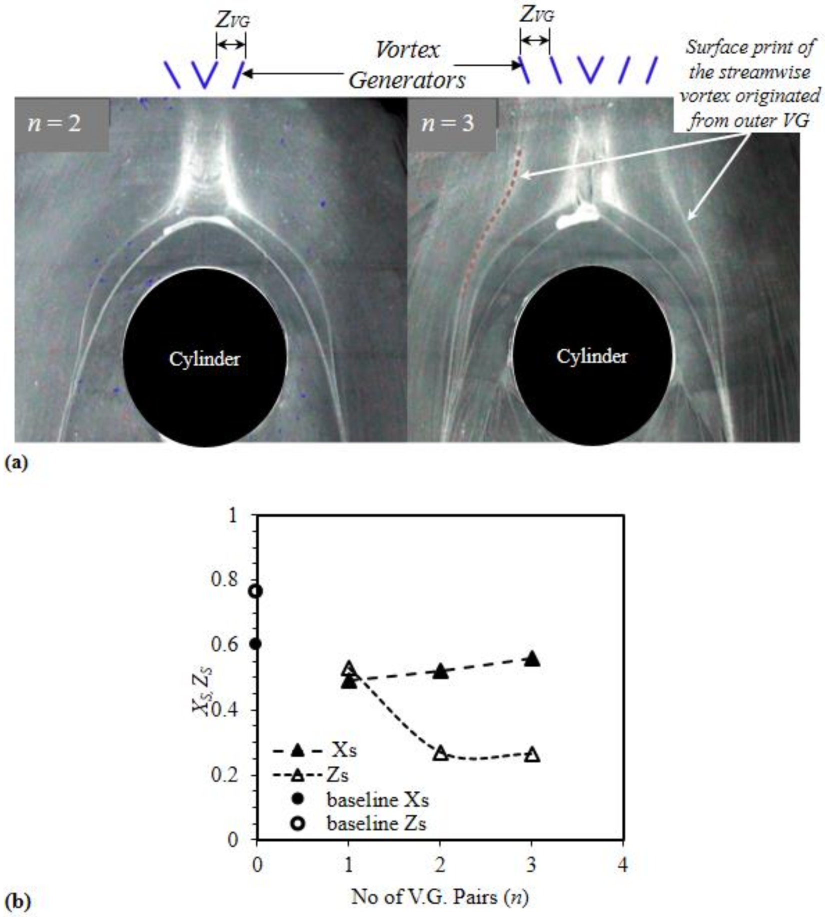

Fig. 7 Effect of parallel arrangement of VG pairs on juncture flow control, (a) Surface oil flow visualization when n = 2 and 3 with Z_{VG} = 4h and (b) separation lengths *Xs* and *Zs* when vortex generators were installed in parallel arrangement at L = *2D* with Z_{VG} = 4*h*.

of the horseshoe vortex under stream wise vortices generated from the vortex generators. The experimentation was done using twenty (20) pressure sensing ports along the upstream symmetric axis covering the length from -1.7D to -0.5D. Effects of all the parameters analyzed using surface oil flow visualization were tested using surface pressure measurements and the details are given in the following text.

3.2.1 Effect of the distance between the leading edge of cylinder to trailing edge of most downstream VG Pair (L) in series arrangement

From the results of the surface oil flow visualization it is shown that the gap "*L*" plays a very important role in reducing the separation length upstream (X_S) of the juncture. Surface pressures (C_P, shown in Fig. 8) were measured for single (n = 1) and multiple (n = 2 and 3) low drag VG pairs arranged in series for L = *D, 2D and 3D* for fixed S_{VG} = 0 and compared with baseline (without control) case.

From Fig. 8(a) it is observed that, for the base line case as the flow approaches the cylinder leading edge at X = -0.5*D*, the boundary layer flow experiences the adverse pressure of the cylinder. The pressure (C_P) gradually rises till X = -0.9*D* (Fig. 8(a)) and then dips down and reaches a relatively lower value at X = -0.78*D*. The dip in C_P corresponds to the primary vortex with vortex core at X = -0.78*D* (Baker 1980). C_P monotonically rises beyond this point till the cylinder leading edge, close to which (X = -0.53*D*) maximum values of C_P (= 0.93) was measured.

Comparing the results of the baseline case to those with the control applied, it is observed that for n = 1 (Fig. 8(a)) when the VG are placed at L = D, the dip (corresponds to primary vortex core) moves upstream (X = -0.86*D*) with lower C_P (= 0.3) compare to the baseline case. This shows that the separation length (*Xs*) elongates upstream along the symmetric axis, the same is observed in Fig. 4(a) for n = 1, where X_S = 0.77 is observed compare to X_S = 0.6 for the baseline case. From this point the pressure inclines and reaches C_P = 0.87 close to the leading edge of the cylinder. A hump in C_P between $-1.7 \leq X \leq -1.5$ is due to the presence of VG pairs at this location for L = D in Figs. 8(a)-8(c).

For L = *2D*, a slight dip in C_P is observed close to the cylinder (X = -0.7*D*) after which a gradual rise takes C_P to a maximum value of C_P = 0.75). C_P profile exhibits a very similar behavior when L is increased from L = *2D* to *3D*. Surface oil flow also shows a similar value of X_S for n = 1 when placed at L = 2*D* (X_S = 0.57) and *3D* (X_S = 0.53).

For n = 2 and L = D (Fig. 8(b)), the dip in C_P (corresponding to primary vortex core) moves downstream

(X = -0.71D) compare to the baseline case (X = -0.78D). The maximum C_P (= 0.78) is observed for this case compare to C_P = 0.87 for n = 1 and L = D. Though the strong adverse pressure region has shrunk, the pressure gradient was similar to that of the baseline case. Placing the VG pairs to L = 2D, monotonic rise in C_P was observed. No dip in C_P is observed, rather a leveling of C_P profile is seen for -0.71 ≤ X ≤ - 0.65, and corresponds to the location of the vortex (Baker 1980). This is possibly due to oscillatory nature of the vortex structure (smoothing effect of horseshoe vortex, Dargahi 1989). When n = 3 for L = D (Fig. 8(c)), the dip in C_P (which is observed for both n = 1 and 2) has vanished instead C_P slightly decreases from C_P = 0.53 (*X = -0.71) to* C_P = 0.5 (*X = -0.65)* and then rises to a maximum C_P = 0.67 (*X = -0.53)*. For L = 2D, C_P rises monotonically with a levelling observed for -0.71 ≤ X ≤ - 0.59 and then rises to a maximum C_P = 0.76 close to the cylinder. For L = 3D, a monotonic increase in C_P is observed with leveling for -0.71 ≤ X ≤ - 0.65. C_P then rises and reaches C_P = 0.78 at X = -0.53.

3.2.2 Effect of the shape of the vortex generators in series arrangement

From the surface oil flow visualization it is observed that more or less both triangular and low drag VGs have the similar control effect. This was clearly depicted in the results from Fig. 4 for all the cases, though slight differences were observed when L = D and n = 1 and 2. For pressure measurements, both triangular and low profiles VGs were analyzed for L = 2D, S_{VG} = 0, and n = 1, 2 and 3, the results are plotted in Fig. 9.

From the surface oil flow visualization it is observed that both X_S and Zs are approximately same for both low drag and triangular VGs for all "n". Surface pressure measurements in Fig. 9 also show that for all n (= 1, 2 and 3) both triangular and low drag VGs have similar C_P profiles. This also confirms that both VGs have similar control effect when one, two and three pairs were used in series.

3.2.3 Effect of the spacing between the two vortex generators in a pair (g) (series arrangement)

The gap g = h between the two vortex generators is observed elongating the upstream separation length (X_S) due to the formation of a beak like surface print compare to the when g = 0. Other than the surface structure along the upstream symmetric axis and its close vicinity, the rest of the pattern is observed similar (Please see Fig. 5(a)). The surface pressure measurements show a similar C_P profiles for g = 0 and h, when n=1 (Fig. 10(a)). A dip in C_P is still present but moves close to the cylinder compared to the baseline. Though the separation region is longer for g = h compare to when g = 0 (Fig. 5(a)), the C_P profile shows no difference when n = 1. When n = 2 and 3 (Figs. 10(b) and 10(c)), C_P profiles show slight differences in the region where smoothing is observed. The difference is larger in case of n = 2 compared to n = 3. The maximum C_P in both the cases (n = 2 and 3) though is similar for both g = 0 and h. The pressure gradient is observed least for n = 2 and g = 0 shown in Fig. 10(b).

3.2.4 Effect of the streamwise gap between two VG pairs (S_{VG}) when arranged in series

Surface oil flow results shows that S_{VG} has no effect on the separation length X_S (please see Fig. 6). Similar observations are also made from the surface pressure measurements (C_P), as plotted in Fig. 11. Monotonic rise in C_P is observed for all S_{VG} (= 0, 2h and 4h) values used in the study for both n = 2 and 3. The only difference in the two cases (n = 2 and 3) is that of the maximum C_P value, which is C_P = 0.74, 0.72 and 0.74 when S_{VG} = 0, 2h *and 4h* respectively for n = 2, increase to C_P = 0.77, 0.77 and 0.75 when S_{VG} = 0, 2h *and 4h* and n = 3. It is concluded from the results obtained that two pairs of vortex generators (*n = 2*) arranged in series with any gap S_{VG} = 0, 2h and 4h can be used in the optimal arrangement.

3.2.5 Effect of the lateral gap between two co-rotating VGs on either side of symmetric axis (Z_{VG}) when arranged in parallel

The effect of gap (Z_{VG}) between the VGs when arranged in parallel on the surface pressure measurements is evaluated for Z_{VG} = 2h and 4h as shown in Fig. 12. Only two VGs (n = 2) arrangement is evaluated and results of C_P distributions are plotted in Fig. 12.

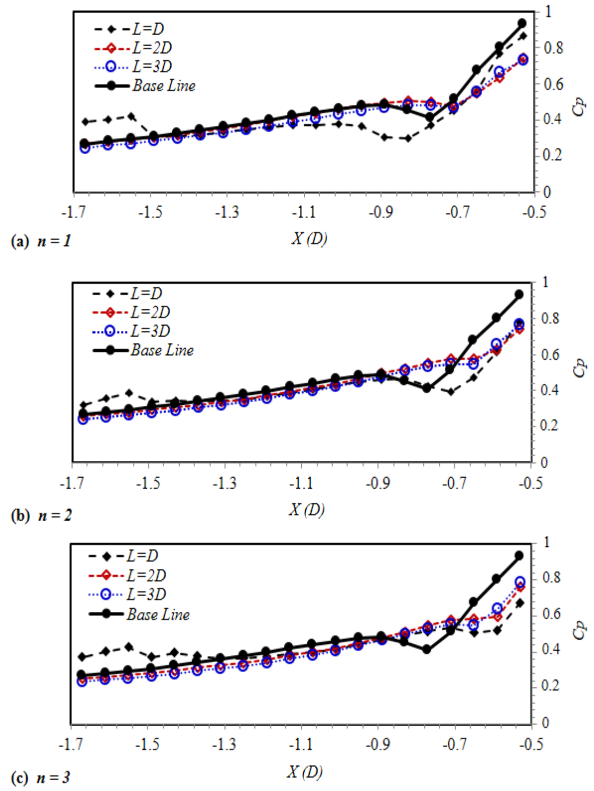

Fig. 8 Surface pressure (C_P) measurements along the symmetric axis for different gaps (L) between VG pairs and cylinder, for low drag vortex generators with fixed S_{VG} = 0, (a). Single VG pair, (b) Two VG pairs, and (c) three VG pairs arranged in series

It is observed that streamwise vortex from third VG in three VGs (n = 3) arrangement bypasses the juncture region and interacts with legs of horseshoe vortex downstream of the juncture (Please see Fig. 7(a)) so not discussed for surface pressure measurements. Fig. 12 shows that the gap Z_{VG} has significant effect on the C_P distribution along the upstream symmetric axis. $Z_{VG} = 4h$ has dip in C_P at location ($0.79 \leq X \leq 0.71$) similar to that of baseline case but has leveling effect. For $Z_{VG} = 2h$ on the other hand the dip (X = 0.65) moves closer to the cylinder, this shows that the separation region has reduced. A small dip on the other hand shows a rather weak horseshoe vortex compared to the baseline as well as $Z_{VG} = 4h$ case. The maximum C_P for both Z_{VG} = 2h and $Z_{VG} = 4h$ is the same C_P = 0.72.

4. Conclusions

In the study a number of arrangement parameters of passive vortex generators (VG) are applied to reduce the juncture flow. Two shapes of the VGs, namely, triangular and low drag profile are used in common flow up configuration. A number of parameters depending upon the arrangement of the single and multiple VG pairs are

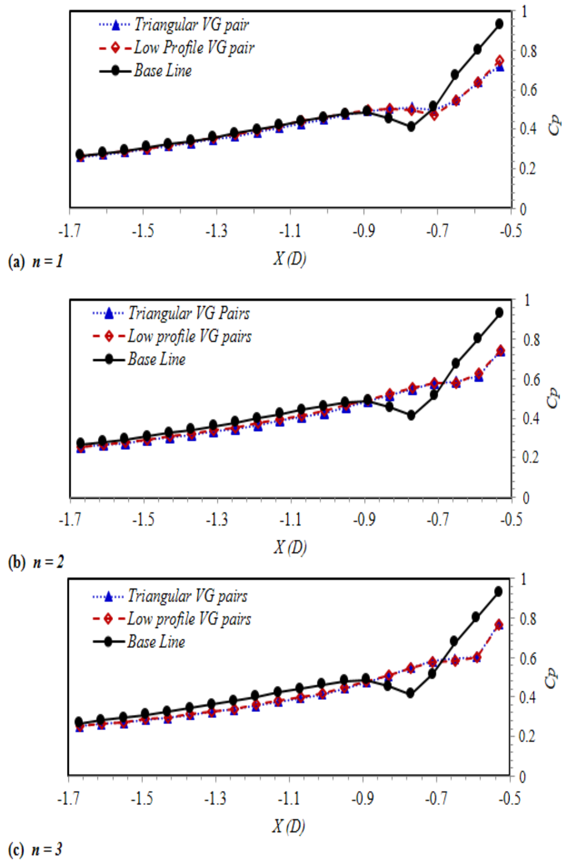

Fig. 9 Effect of shape of the VG pairs on the plate surface pressure distribution along upstream symmetric axis, (a). Single VG pair, (b) Two VG pairs arranged in series, and (c) Three VG pairs arranged in series

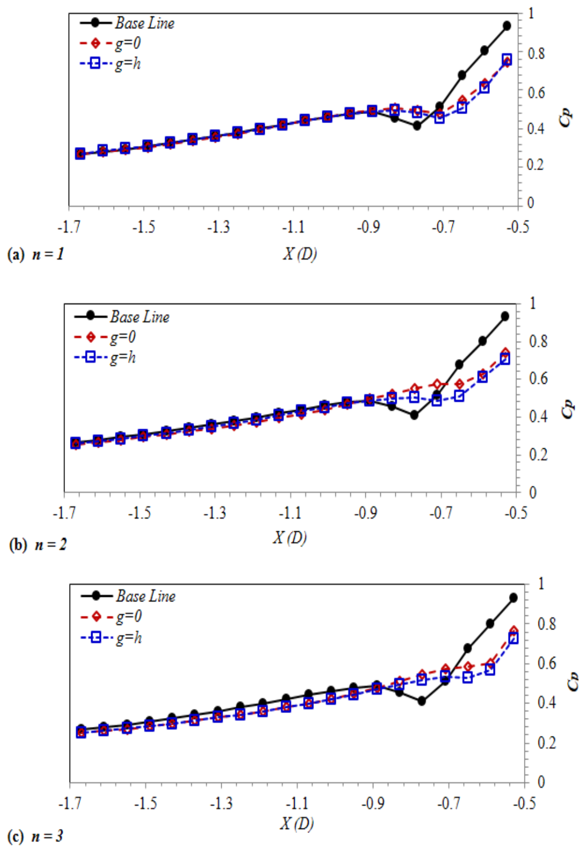

Fig. 10 Effect of the gap between the vortex generators in a pair (g) on surface pressure distribution (C_P) upstream of juncture, (a) single pair, (b) two pairs in series and (c) three pairs in series

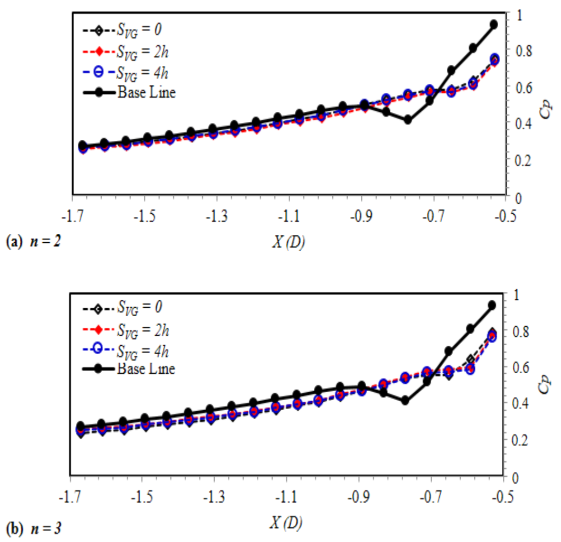

Fig. 11 Effect of gap (S_{VG}) between two VG pairs when arranged in series on surface pressure (C_P) distribution along upstream symmetric axis (L = $2D$), (a). Two VG pairs, and (b) Three VG pairs

evaluated for the control effect. The following conclusions are drawn from the study.

- The horseshoe vortex can be suppressed using a counter rotating pair of streamwise vortices generated by the two vortex generators in common flow up configuration.
- Both triangular and low drag VGs are observed having similar control effect on the horseshoe vortex control. Comparable reduction in separation region and in the adverse pressure gradients are observed for both shapes of vortex generators.
- Parametric study shows that multiple VG pairs arranged in series upstream of juncture improves the effectiveness of the control method. The distance L plays important role in reducing the upstream separation length (X_S), maximum effectiveness is observed when L = 2D. It is observed that no significant difference in control effect is observed with variation in streamwise spacing (S_{VG}) when multiple VG pairs are used in series. Increasing the number of VG pairs to n =3 and 4, neither the separation region nor the adverse pressure gradient reduces significantly compare to n =2. Two low drag VG pairs (n =2) at L = 2D and g = 0, in series arrangement provides the best control effect in current study.
- Parallel arrangement does not show significant control effect in the upstream symmetric region, the control is rather palpable on both sides. Varying the span-wise spacing between two co-rotating vortex generators (Z_{VG}) shows that the streamwise vortices generated by VG placed with small spacing (Z_{VG} = 2h) may interfere with each other thus loose some of their strength on flow control. While for wide spacing (Z_{VG} = 4h) they might be too wide to interact with the juncture flow in the upstream region thus of no use to horseshoe vortex control.

Acknowledgments

First author acknowledges the great support of Mr. Wu Xing Gang who helped him in conducting the experiments. The second author wants to acknowledge the support from NSFC Project no 11372027 and 10872022.

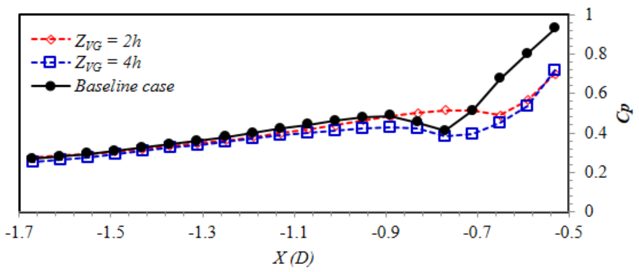

Fig. 12 Effect of gap (Z_{VG}) between two VG pairs when arranged in parallel on surface pressure (C_P) distribution along upstream symmetric axis, L = 2D, n = 2

References

Andoh, M., Motosuke, M. and Honami, S. (2009), "Interaction of longitudinal vortex with horseshoe vortex configuration effect of longitudinal vortex", *Proceedings of the 39th AIAA Fluid dynamics conference*, San Antonio, Texas, USA, June.

Andoh, M., Motosuke, M. and Honami, S. (2010), "The interaction between horseshoe vortex and longitudinal vortices from the votex generator", *Proceedings of the ASME Turbo Expo, Power for Land Sea and Air*, Glasgow, UK.

Baker, C.J. (1980), "The turbulent horseshoe vortex", *J. Wind Eng. Ind. Aerod*., **6**, 9-23.

Bijan, D. (1990), "Controlling mechanism of local scour", *J. Hydraul. Eng*. - *ASCE*, **116**(10),1197–1214.

Bloxham, M., Hollis, R. and Bons, J. (2008), "Horseshoe vortex control with leading edge endwall boundary layer removal", *Proceedings of 4TH Flow Control Conference*, Seattle, Washington, USA, June.

Bons, J., Benton, S., Bernardini, C. and Bloxham, M. (2018), "Active flow control for low-pressure turbines", *AIAA J.* (Volume, Issue and page number not assigned yet).

Dargahi, B. (1989), "The turbulent flow field around a circular cylinder", *Exp. Fluids*., **8**(1-2), 1-12.

Devenport, W.J., Agarwal, N.K., Dewitz, M.B., Simpson, R.L. and Poddar, K. (1990). "Effects of a fillet on the flow past a wing body junction", *AIAA J.*, **28**(12), 2017-2024. https://doi.org/10.2514/3.10517.

Doerffer, P., Flaszynski, P. and Magagnato, F. (2003), "Streamwise vortex interaction with a horseshoe vortex", *J. Therm. Sci*., **12**(4), 304-309.

Gupta, A.K. (1987), "Hydrodynamic modification of the horseshoe vortex at a verticle pier junction with ground", *Phys. Fluids*, **30**(4), 1213-1215. https://doi.org/10.1063/1.866270.

Honami, S., Andoh, M., Tanabe, S. and Motosuke, M. (2011), "Effects of co-rotating longitudinal vortices in turbulent structures in the leg of horseshoe vorticex", *Proceedings of the ASME Turbo Expo*., Vancouver, British Columbia, Canada, June.

Hua, Z., Younis, M.Y., Bo, H., Hong, W. and Xuee, W. (2012), "Investigation of attachment saddle point structure of 3-D steady separation in laminar juncture flow using PIV", *J. Vis.*, **15**(3), 241-252.

Johnson, M.J., Ravindra, K. and Andres, R. (1994), "Comparative study of the elimination of the wing fuselage junction vortex by boundary layer suction and blowing", *Proceedings of the 32nd Aerosace Science Meeting and Exhibition*, Reno, NV. USA, January.

Kairouz, K.A. and Rahai, H.R. (2005), "Turbulent junction flow with an upstream ribbed surface", *Int. J. Heat Fluid Fl.*, **26**(5), 771-779. https://doi.org/10.1016/j.ijheatfluidflow.2005.02.002.

Kang, K.J., Kim, T. and Song, S.J. (2009), "Strengths of horseshoe vortices around a circular cylinder with an upstream cavity", *J. Mech. Sci. Tech*., **23**(7),1773-1778.

Kubendran, L.R. and Harvey, W.D. (1985), "Juncture flow control using leading edge fillets", *Proceedings of the AIAA 3rd Applied Aerodynamics Conference*, Colorado springs, Colorado, USA, October.

Kumar, K.N. and Govardhan, M. (2011), "Secondary flow loss reduction in a turbine cascade with a linearly varied height streamwise endwall fence", *Int. J. Rot. Mach*., 1-16. http://dx.doi.org/10.1155/2011/352819.

Liu, J.H. and Song, C.Y. (2017), "Efficient suction control of unsteadiness of turbulent wing-plate junction flows", *J. Hydrodyn*., **29**(2), 353-360. https://doi.org/10.1016/S1001-6058(16)60745-X.

Liu, Z.H., Xiong, Y., and Cheng, X.T.U. (2014), "The method to control the submarine horseshoe vortex by breaking the vortex core", *J. Hydrodyn.*, **26**(4), 637-645.

Liu, Z.H., Xiong, Y., Wang, Z.Z. and Wang, S. (2010), "Numerical simulation and experimental study of the new method of horseshoe vortex control", *J. Hydrodyn.*, **22**(4), 572-581. https://doi.org/10.1016/S1001-6058(09)60090-1.

Mohamed Gad-el-hak (2006), *Flow Control Passive, Active, and Reactive Flow Management*, Cambridge University Press, Cambridge, UK.

Munson, B.R., Young, D.F. and Okiishi, T.H. (2009), *Fundamentals of Fluid Mechanics*, Wiley India, New Dehli, Dehli, India.

Olcmen, S.M. and Simpson, R.L. (1994), "Influence of Wing shapes on surface pressure fluctuations at wing body junctions", *AIAA J.*, **32**(1), 6-15. https://doi.org/10.2514/3.48283.

Ölçmen, S.M. and Simpson, R.L. (2007), "Influence of passive flow-control devices on the pressure fluctuations at wing-body junction flows", *J. Fluid. Eng. -T ASME*, **129**(8), 1030-1037.

Oudheusden, B.W.V., Steenaert, C.B. and Boermans, L.M.M. (2004), "Attachment-line approach for design of a wing-body leading-edge fairing", *J. Aircraft*, **41**(2), 238-246. https://doi.org/10.2514/1.353.

Philips, D.B., Cimbala, J.M. and Treaster, A.L. (1992), "Suppression of the wing body junction vortex by body surface suction", *J. Aircraft*, **29**(1), 118-122. https://doi.org/10.2514/3.46134.

Seal, C.V. and Smith, C.R. (1999), "The control of turbulent end-wall boundary layers using surface suction", *Exp. Fluids*, **27**(6), 484-496.

Theberge, M.A. and Ekmekci, A. (2017), "Effects of an upsream triangular plate on the wing-body junction flow", *Phys. Fluids*, **29**, 097105. https://doi.org/10.1063/1.5000733.

Wang, J.M., Bi, W.T. and Wei, Q.D. (2009), "Effects of an upstream inclined rod on the circular cylinder flat plate junction flow", *Exp. Fluids*, **46**(6), 1093-1104.

Wang, J.M., Liu, W., Xu, Z.H., Ai, Y.T. and Wang, C.J. (2011), "Study on the control of the wing body juncture horseshoe vortex utilizing venturi tube", *J. Aero. Power*, **26**(11), 2617-2622.

Wei, Q.D., Wang, J.M., Chen, G., Lu, Z.B. and Bi, W.T. (2008), "Modification of junction flows by altering the section shapes of the cylinders", *J. Vis.*, **11**(2), 115-124.

Younis, M.Y., Zhang, H., Hu, B. and Mehmood, S. (2014), "Topological evolution of laminar juncture flows under various critical parameters", *Sci. China Tech. Sci.*, **57**(7), 1342–1351.

Younis, M.Y., Zhang, H., Oo, Z.Z., Muhammad, Z. and Bo, H., (2010), "Control of Juncture flows", *Proceedings of The Asia Pecific International Symposium on Aerospace Technology,* Xian, China, September.

Zess, G.A. and Thole, K.A. (2002), "Computational design and experimental evaluation of using a leading edge fillet on a gas turbine vane", *J. Turbomach.*, **124**(2), 167-175.

AD